

Biodynamic modeling, system identification, and variability of multi-finger movements

Sang-Wook Lee¹, Xudong Zhang*

Department of Mechanical Science and Engineering, University of Illinois at Urbana Champaign, 1206 West Green Street, Urbana, IL 61801, USA

Accepted 27 April 2007

Abstract

A forward dynamic model of human multi-fingered hand movement is proposed. The model represents digits 2–5 in manipulative acts as a 12-degrees-of-freedom (DOF) system, driven by torque actuators at individual joints and controlled using a parsimonious proportional–derivative (PD) scheme. The control parameters as feedback gains along with an auxiliary parameter to modulate the joint torque magnitudes and cross-coupling can be empirically identified in an iterative procedure minimizing the discrepancy between the model-prediction and measurement. The procedure is guided and computationally accelerated by pre-knowledge of relations between the parameters and kinematic responses. An empirical test based on real grasping movement data showed that the model simulated the multi-finger movements with varied inter-joint temporal coordination accurately: the grand mean of the root-mean-square-errors (RMSE) across trials performed by 28 subjects was 3.25°. Analyses of the model parameters yielded new insights into intra- and inter-person variability in multi-finger movement performance, and distinguished the less variable motor control strategy from much more variable anthropometric and physiological factors.

© 2007 Elsevier Ltd. All rights reserved.

Keywords: Forward dynamics; PD control; System identification; Finger movement

1. Introduction

Models of human movements are enabling emerging applications such as digital design and prototyping of human–machine systems and consumer products, and computer-aided surgeries (Delp and Loan, 2000; Zhang and Chaffin, 2005). Despite the importance of the hand in human physical functions, most of the existing models or simulation tools do not feature a realistic representation of the hand, particularly to the level of finger segmental movements.

The existing finger biomechanical models can be generally classified as static and dynamic models. Static models were created mainly for estimating finger muscle and tendon forces during isometric functions or exertions (Valero-Cuevas et al., 1998; Li et al., 2000; Milner and

Dhaliwal, 2002; Sancho-Bru et al., 2003; Pearlman et al., 2004). These models relate, for example, an external force applied at the fingertip to the internal muscle/tendon forces. Static models have also been proposed to predict prehensile configurations or poses (Buchholz and Armstrong, 1992; Lee and Zhang, 2005). They provide a basis for evaluating designs of hand-operated tools or devices, and help gain better understanding of human prehensile behavior (Lee and Zhang, 2005).

Dynamic models of the finger movements are relatively sparse, and are mostly inverse dynamics models, which estimate the muscle/tendon forces given a specification of the finger motions (Brook et al., 1995; Buchner et al., 1988; Sancho-Bru et al., 2001). A forward dynamics or forward solution model is arguably what represents the real sequence of events in movement production: from a neural drive, to muscle forces, to time-varying joint torques, and then to the acceleration or deceleration of the body segments (Winter, 2004). Currently, a true forward dynamics model for predicting or simulating multi-fingered hand movements is lacking. Models that drive simple

*Corresponding author. Tel.: +1 217 265 8031; fax: +1 217 244 6534.

E-mail address: xudong@uiuc.edu (X. Zhang).

¹Rehabilitation Institute of Chicago, 345 E. Superior St., Chicago, IL 60610, USA

robotic hand manipulation typically miss important human multi-fingered hand movement characteristics such as temporal coordination patterns of individual joint flexions within a digit (Darling et al., 1994; Holguin et al., 1999; Braido and Zhang, 2004). On the other hand, a neural-command- or muscle-driven forward dynamic model for multi-fingered hand movement, as those developed for simulating full-body walking (Anderson and Pandy, 2001), would incur tremendous computational cost. The potential for real-time simulation as demanded by the aforementioned applications is limited.

In this work, we propose a new forward dynamic model that can facilitate computationally efficient simulation of multi-fingered hand movements. This model incorporates torque-driven forward dynamics and a parsimonious parametric proportional–derivative (PD) controller, while the cross-coupling in joint torques within each digit is compactly represented by an auxiliary constraint parameter. An iterative parameter identification scheme, guided by observed relationships between the parameters and kinematic responses, efficiently estimates the model parameters from experimental data. As we evaluate the model performance experimentally, we also seek insights into the movement variability, in terms of inter-person versus intra-person variability, and variability in the motor control versus in the plant.

2. Methods

2.1. Linkage representation and torque-based dynamics

In the proposed model, each of digits 2–5 is represented as an open chain of three rigid segments connected through three one-degree-of-freedom (1-DOF) revolute joints (Fig. 1). The metacarpophalangeal (MCP) joint is generally modeled as a 2-DOF joint (An et al., 1979). Our model in the present form considers only the flexion–extension not the abduction–adduction of MCP.

The finger segments are represented as conical cylinders with density of $1.1(\text{g}/\text{cm}^3)$ (Dempster, 1955), and the length and thickness of each segment are modeled as functions of the hand length (Lee and Zhang, 2005). The equation of motion governing the dynamics of the 3-DOF system is presented in Appendix A.

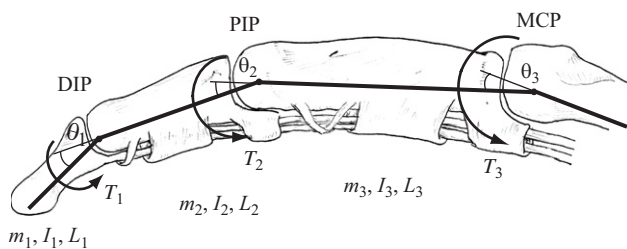


Fig. 1. A three-segment 3-DOF linkage representation of a digit (any of digits 2–5). Each segment is flexed or extended by the torque actuator at its proximal joint. Joints 1–3 are the distal interphalangeal (DIP) joint, proximal interphalangeal (PIP) joint, and the metacarpophalangeal (MCP) joint, respectively; segments 1–3 are the distal phalanx, the middle phalanx, and the proximal phalanx; m_i , I_i , and L_i represent the mass, inertia property, and length of a segment. Each finger segment is actuated by three torque generators (τ_1 , τ_2 , and τ_3), which represents the total actions of the musculotendons required to produce finger joint flexion and extension.

2.2. Controller model of the finger dynamic system

A PD control scheme is proposed to control the biodynamic system. The torque at joint i , τ_i , is related to joint angle position and angular velocity as the following:

$$\tau_i = -K_i^p(\theta_i - \theta_i^f) - K_i^d(\dot{\theta}_i - \dot{\theta}_i^f), \quad (1)$$

where θ_i denotes the flexion angle of joint i , θ_i^f the joint angle in the terminal grip posture, K_i^p and K_i^d the proportional and derivative feedback gains of joint i , respectively; K^p characterizes the controlled dynamic stiffness that determines the movement speed, while K^d considers the velocity feedbacks of muscles and their reflex (Gottlieb and Agarwal, 1979).

2.3. Auxiliary parameter constraining joint torque ratio

An auxiliary parameter modulating the magnitudes of individual finger joint torques is a key and novel feature in the proposed model. If a simple PD control scheme as described in Section 2.2 were applied to the multi-link system, the resulting movements would be of different characteristics from those of actual human movements. First, the movement would reach peak velocity too soon, resulting in highly left-skewed angular velocity profiles, in contrast to the typical symmetric bell-shaped velocity profiles observed in human movements. This was found to be one of the deficits of equilibrium-point-hypothesis models (Hatsopolous, 1994), which assume a mathematical representation akin to Eq. (1). Second, three joints of each digit would have nearly simultaneous movement onsets, contradicting the observation that in real human hand movements, small but noticeable time leads or lags exist between onsets of different finger joints (Holguin et al., 1999; Braido and Zhang, 2004).

The above described natural characteristics of finger movements may be considered as a result of the combined effects of flexor tendons crossing multiple joints, the intricate finger extensor mechanism (Valero-Cuevas et al., 1998) and passive joint characteristics (Kamper et al., 2002); these mechanisms modulate the joint torque production, and determine their relative magnitudes within each digit accordingly. Due to such constraints on joint torques in movement initiation phase, even if the neural commands could arrive simultaneously, corresponding temporal lead or lag patterns in joint flexions would emerge. Such patterns would be specific to both subjects' physiological conditions and movement types, which define and alter the mechanisms of joint torque regulation.

Therefore, a maximum torque ratio vector \underline{M}^{\max} , which represents the relative magnitudes of the torque values generated in three joints, is introduced as an auxiliary parameter and incorporated into the model to compensate the limitation of the proposed model structure:

$$\underline{\tau} \leq \underline{M}^{\max} \quad \text{where } \underline{\tau} = [\tau_1 \quad \tau_2 \quad \tau_3], \quad \underline{M}^{\max} = [M_1^{\max} \quad M_2^{\max} \quad M_3^{\max}]. \quad (2)$$

By directly constraining the relative magnitudes of peak torque values, this parameter simulates the effect of cross-coupling in joint torque generations in a condensed manner. The M^{\max} does not correspond to the actual joint strength limit, in which case factors such as the force–velocity relationship would need to be considered.

2.4. Control parameter estimation

The parameters of the proposed control structure can be estimated by a system identification procedure minimizing the discrepancy between the model-reproduced and measured joint angles. This discrepancy is quantified as the difference between two sets of kinematic descriptors for measured and model-reproduced finger joint profiles. Three descriptors compactly capture the kinematics of each finger DOF: the rise time T^{rise} and peak velocity time T^{peak} jointly characterize the spatial–temporal pattern, and the movement initiation time T^{init} specifies the temporal coordination among multiple joint flexions. Here, T^{rise} is defined as the time to rise from 5% to 95% of the total angular displacement, T^{peak} the time from T^{init} to when the joint angular velocity reaches its maximum, and T^{init} the time a joint takes to reach 5% of its total displacement.

In determining these descriptors from measured finger joint kinematics, a common reference time point is needed and could simply be set at the beginning of recording.

The kinematic descriptors are under the influence of the three parameters in the proposed controller. K^p primarily adjusts the movement speed, which affects T^{rise} ; K^d modifies the damping characteristics of the system and primarily determines T^{peak} . Thus, the shape of an angular profile is essentially determined by these two gain parameters. In addition, the overshoot in the response is also modulated by K^d . M^{max} defines the relative magnitudes of three joint control torques within a digit in generating a given movement, and regulates the temporal coordination of the movements of three segments (T^{init} values relative to each other). A pilot analysis was performed on a representative three-link system approximating the finger linkage system, and the above postulated relations were verified. These relations serve to guide and accelerate the following search routine for estimating the dynamic control parameters.

An iterative search routine was devised to estimate the control parameter values (Fig. 2). This search process continues until the RMSE values of all angular profiles become less than a preset threshold (3°). The search process also terminates when the solution does not exhibit any improvement (i.e., RMSE values are not decreased) after three iterations.

2.5. Experimental data

The modeling approach was tested using data from an experiment in which 28 anthropometrically diverse participants performed right-handed motions of grasping a vertically oriented cylindrical handle of 45 mm in diameter. Reflective markers (5 mm in diameter) were attached on the dorsum of the subjects' right hand at 21 surface landmarks. A five-camera Vicon 250 motion capture system recorded the reflective marker coordinates at a sampling frequency of 120 Hz during the grasping motions, and then exported the time histories of three-dimensional (3D) coordinates, from which finger joint angles were calculated. The joint

angular profiles were filtered using a low-pass Butterworth filter with a cut-off frequency of 20 Hz.

2.6. Analysis of correlation between model parameters and movement characteristics

An analysis was performed to verify some anticipated relationships between the model parameters and dynamic characteristics of the motions. Specifically, we analyzed how movement speed and kinetic energy are correlated with the model parameters. The kinetic energy profiles were found to be indicative to changes in finger inter-segment or -joint coordination and dynamics (Kuo et al., 2006).

We defined the index of maximum rotational kinetic energy (KE) of the i th segment in the digit j as

$$KE_{i,j} = \frac{1}{2} I_{i,j} \omega_{i,j}^{peak^2}, \quad (3)$$

where $I_{i,j}$ is the inertia, and $\omega_{i,j}^{peak}$ is the peak angular velocity of the i th segment of digit j .

The total maximum rotational kinetic energy (TKE) of the digit j is

$$TKE_j = \sum_{i=1}^3 KE_{i,j}. \quad (4)$$

The work index of a finger segment (WI), and the total work index (TWI) of a digit, respectively, are:

$$WI_{i,j} = M_{i,j}^{max} [\theta_{i,j}^f - \theta_{i,j}^0] \quad \text{and} \quad (5)$$

$$TWI_j = \sum_{i=1}^3 WI_{i,j}, \quad (6)$$

where $M_{i,j}^{max}$ is the maximum torque parameter value, $\theta_{i,j}^f$ is the final angle, and $\theta_{i,j}^0$ is the initial angle of the i th segment of digit j . This work index provides an upper bound for the work done during the flexion by a

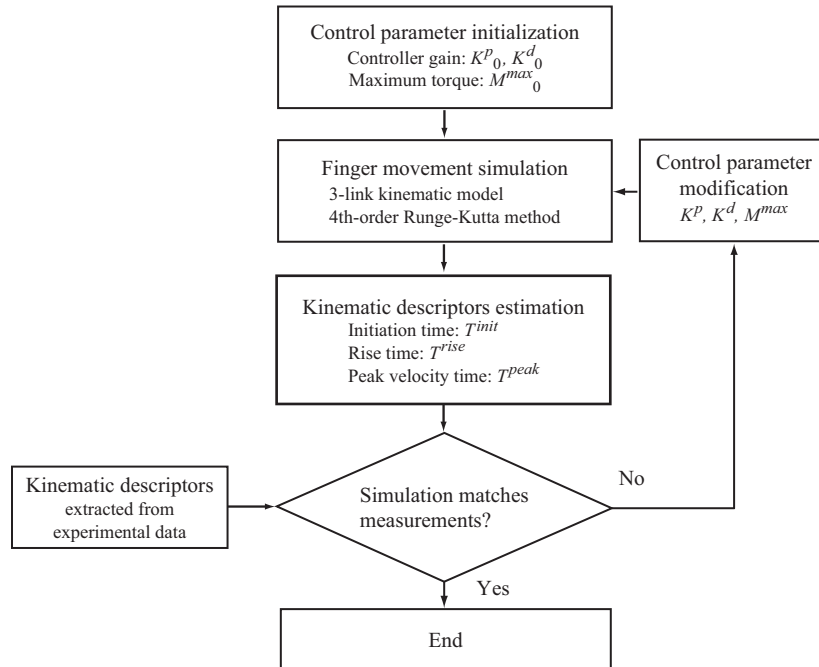


Fig. 2. A logic diagram of the iterative search routine for estimating the model parameters for a measured movement. In each iteration, for the generated movement given a parameter set, the kinematic descriptors were calculated and compared with those obtained from experimental data. For each joint, the shape of profile was modified by adjusting its K^p and K^d gain; K^p of the model was adjusted in 5% increments if T^{rise} of the simulated profile is larger than that of experimental data, and vice versa. The K^d gain was adjusted also in 5% increments by comparing the T^{peak} . M^{max} values were adjusted based on the T^{init} values of the simulated and experimental data; for example, if T^{init} of a simulated angular profile was larger than that of experimental data (if the simulated joint flexion starts slower than experimental data), the M^{max} value of the corresponding joint was adjusted up in 3% increments.

segment or multiple segments, computed by taking time integrals of the product of time-varying torque and joint angle values.

The intra- and inter-person variabilities of the estimated control parameters (K^p , K^d , and \underline{M}^{\max}) were analyzed. The intra-person variability V_{intra} of the estimated parameter is defined as the pooled estimate of the intrinsic variation in the movement-specific parameter values obtained for each person:

$$V_{\text{intra}} = \sqrt{\frac{1}{N_{\text{sub}}} \sum_{k=1}^{N_{\text{sub}}} \sum_{i=1}^{N_{\text{trial}}} \frac{1}{N_{\text{trial}} - 1} (P_i^k - \bar{P}^k)^2},$$

$$\bar{P}^k = \frac{\sum_{i=1}^{N_{\text{trial}}} P_i^k}{N_{\text{trial}}}, \quad (7)$$

where N_{sub} is the number of the subjects (28), N_{trial} is the number of repeated trials (2), and P_i^k is the parameter value of subject k in trial i . The inter-person variability V_{inter} is defined as the variation of the parameter averages across all individuals considered:

$$V_{\text{inter}} = \sqrt{\frac{1}{N_{\text{sub}} - 1} \sum_{k=1}^{N_{\text{sub}}} N_{\text{trial}} (\bar{P}^k - \bar{\bar{P}})^2},$$

$$\bar{\bar{P}} = \frac{1}{N_{\text{sub}}} \sum_{k=1}^{N_{\text{sub}}} \bar{P}^k. \quad (8)$$

The V_{intra} here is equivalent to the ‘within-subject variance’ in a conventional analysis of variance (ANOVA), and the V_{inter} to the ‘between-subject variance.’

3. Results

The simulated grasping movements, corresponding to the estimated parameters yielded from the iterative routine, agreed well with the original experimental data (Fig. 3). The root-mean-square-error (RMSE) values, quantifying the differences between the model-reproduced and measured angular profiles for each joint, ranged from 2.70° to 3.62° (grand mean = 3.25° for all subjects). Different same-digit joint motion initiation sequences were observed in the experimental data, and distinguished by the model (Fig. 4): the MCP–proximal interphalangeal (PIP)–distal interphalangeal (DIP) sequence was dominant, and counted for 86% of the total.

The magnitudes of estimated K^p , K^d , and \underline{M}^{\max} display similar patterns (Fig. 5): across digits, the relative magnitudes of parameters for the same joints seem to reflect the size differences of digits; across three joints with digits, reflect the size differences of segments distal to the respective joints.

The K^p value was found to be well correlated with movement speed measured by squared peak velocity ω^{peak^2} ($R: 0.784\text{--}0.956$, mean = 0.890 ; Fig. 6 and Table 1), while the K^d value had a more moderate correlation with ω^{peak^2}

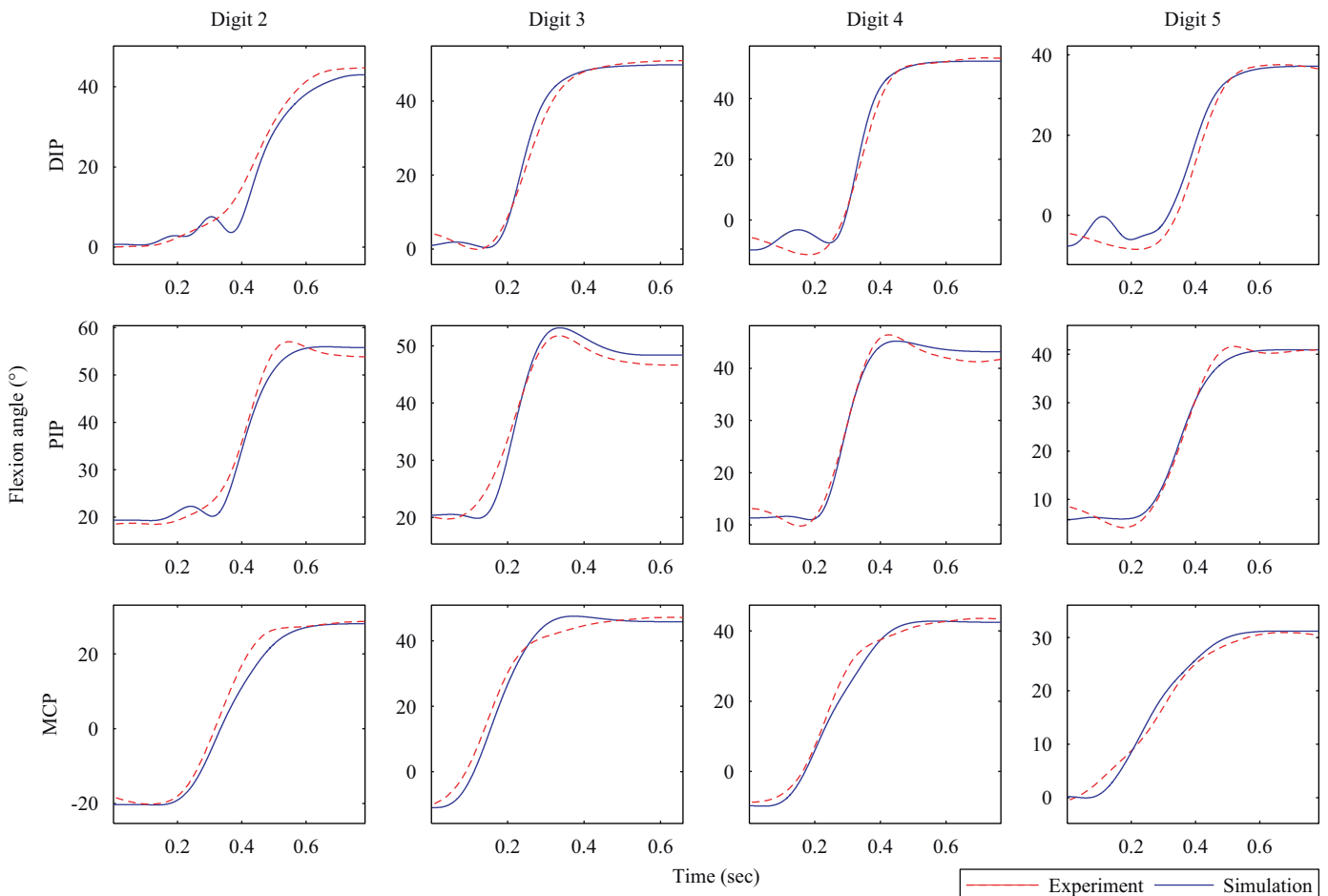


Fig. 3. A representative comparison of measured versus model-simulated joint angle profiles.

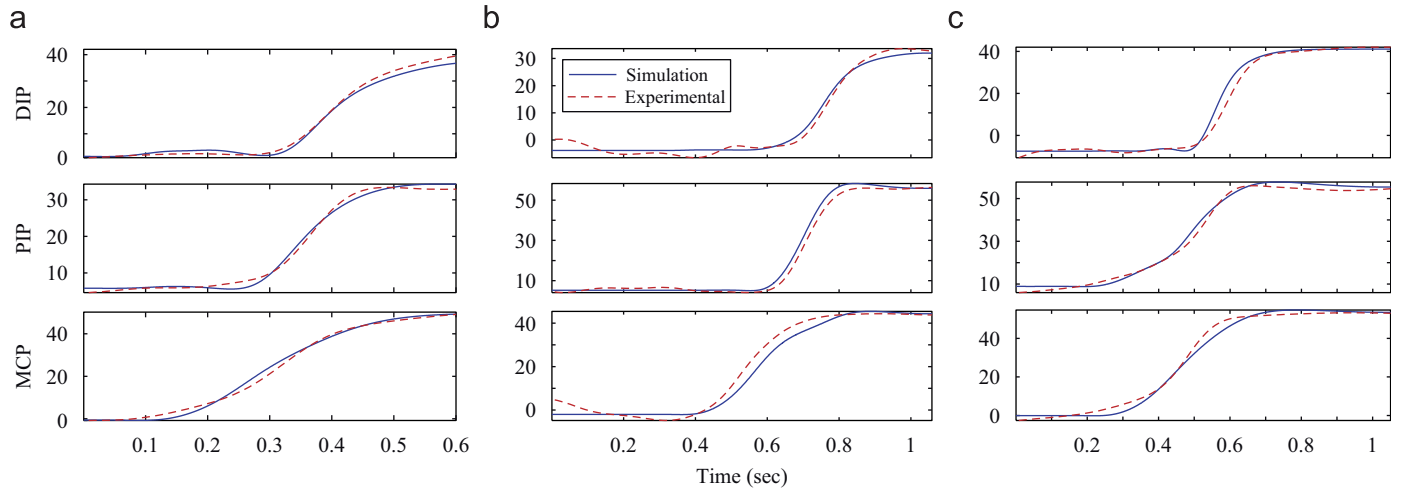


Fig. 4. Comparisons of the experimental (dashed) and simulated (solid) angular profiles of the grasping movements for three representative cases of different onset sequences: (a) MCP-PIP-DIP (most typical), (b) PIP-MCP-DIP, and (c) MCP-DIP-PIP.

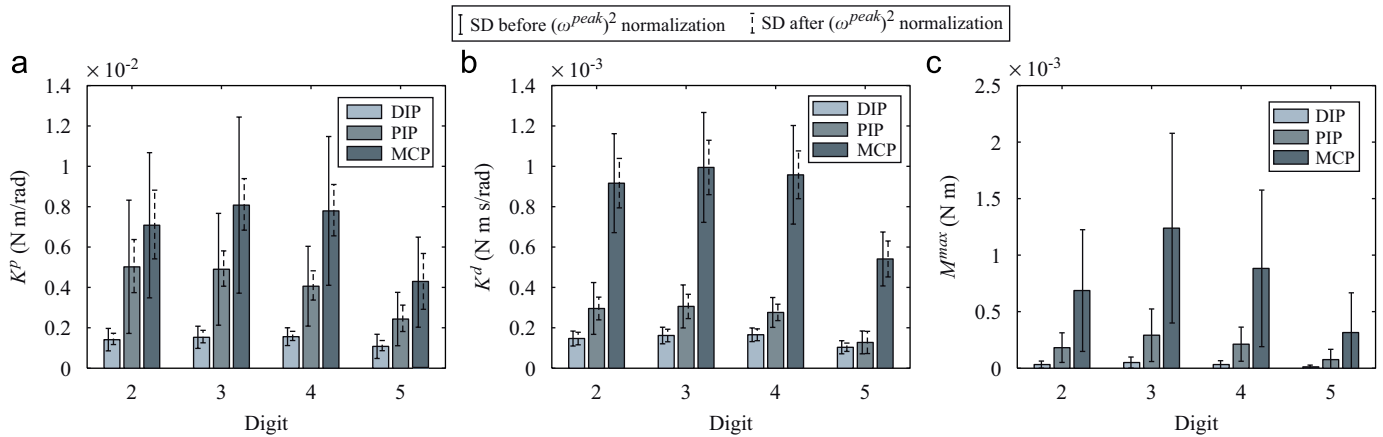


Fig. 5. Mean and standard deviation values of the estimated model parameters: (a) K^P , (b) K^d , and (c) M^{\max} .

(mean $R = 0.623$). To remove the effects of subject-specific movement speed on the K^P and K^d values, these parameters were normalized by the ω^{peak^2} . The variation in the K^P and K^d values was significantly reduced by the normalization: the range of reduction in standard deviation was 44–71% for K^P , and 3–56% for K^d (see Fig. 5(a) and (b)).

The M^{\max} value of each joint did not have much correlation with any of independent variables ($R < 0.500$). The correlation between kinetic energy (KE) and work index (WI) of each joint was moderate (mean $R = 0.646$), but a higher correlation between total kinetic energy (TKE) and total work index (TWI) was observed (mean $R = 0.876$). Of note is that the kinetic energy is a function of the moment of inertia, and thus is associated with the segmental mass and length.

The variability analysis revealed that V_{inter} was comparable to or slightly greater than the V_{intra} for the normalized K^P and K^d values: for normalized K^P (Table 2), the $V_{\text{intra}}/V_{\text{inter}}$ ratios varied from 0.71 to 1.86 across all joints, with a mean of 1.116; for normalized K^d (Table 3), the

ratios varied from 0.77 to 1.85, with a mean of 1.27. In contrast, V_{inter} values for M^{\max} were much greater than V_{intra} values (Table 4); $V_{\text{inter}}/V_{\text{intra}}$ ratios ranged from 1.59 to 3.10, with a mean of 2.065.

4. Discussion

In this work, a new biomechanical model of multi-finger movements, incorporating computationally tractable forward dynamics and system identification, is presented. The proposed model has an open architecture with parameters that can be empirically estimated from movement data. Once these parameters are known, the model enables a time-efficient simulation of multi-finger movements via forward dynamics controlled by a parsimonious PD scheme. Our empirical test showed that the model was capable of replicating multi-fingered grasping movements accurately. In particular, natural finger movement characteristics, such as different onset times of joint flexions and sigmoidal shapes of angular profiles, were well captured (Figs. 3 and 4).

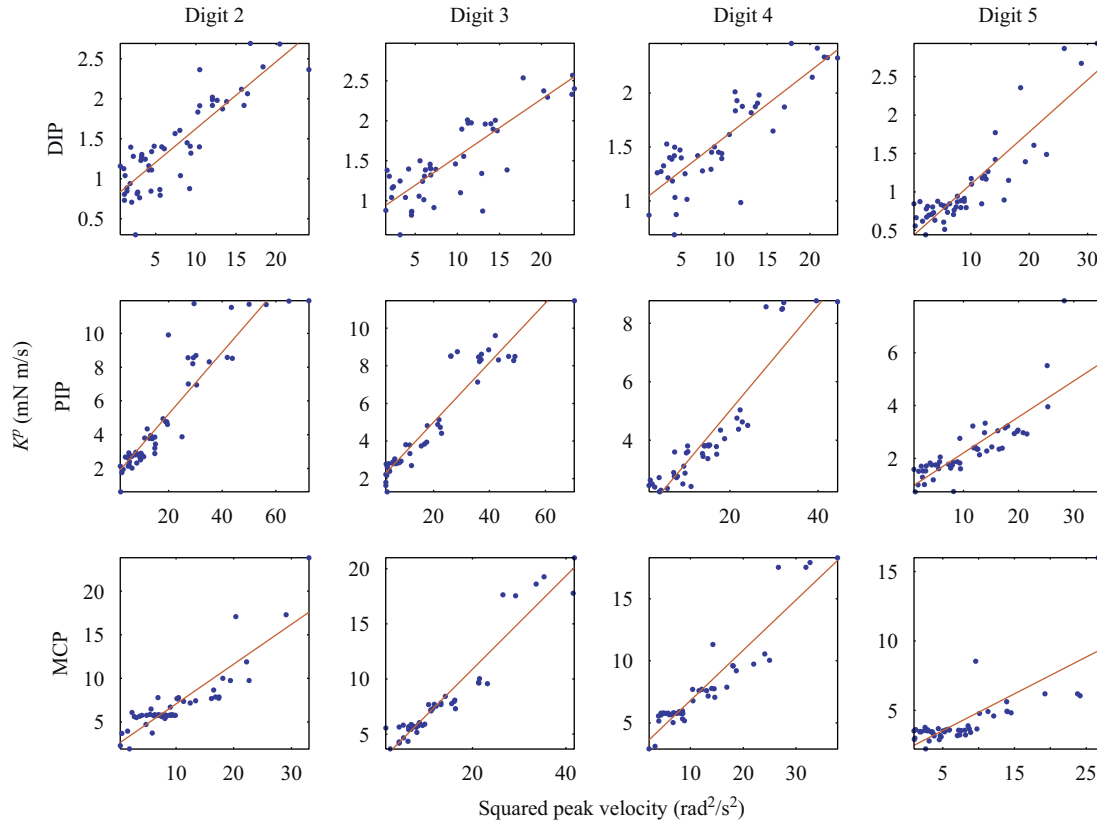


Fig. 6. Correlation between K^P and the squared peak velocity. The grand mean value of the coefficient of correlation (R) values was 0.890.

Table 1
Coefficient of correlation (R) values between K^P and ω_{peak}^2

	Digit			
	2	3	4	5
DIP	0.866	0.828	0.855	0.907
PIP	0.917	0.949	0.930	0.869
MCP	0.881	0.956	0.938	0.784

Table 2
Intra- and inter-person variability of the normalized K^P values (unit: 10^{-3} N m/rad)

	Intra-person variability				Inter-person variability			
	Digit				Digit			
	2	3	4	5	2	3	4	5
DIP	0.282	0.266	0.185	0.144	0.248	0.318	0.191	0.268
PIP	1.133	0.703	0.684	0.644	1.628	0.832	0.717	0.455
MCP	1.566	1.110	0.983	1.433	1.944	1.069	1.054	1.101

The proposed model structure may be likened to the multi-level functional hierarchy for human motor control (Todorov, 2004). The controller model is intended to represent the ‘higher-level’ control of multi-finger movements by tuning the active joint stiffness and damping,

Table 3
Intra- and inter-person variability of the normalized K^d values ($\times 10^{-3}$ N m s/rad)

	Intra-person variability				Inter-person variability			
	Digit				Digit			
	2	3	4	5	2	3	4	5
DIP	0.027	0.028	0.021	0.013	0.032	0.034	0.027	0.024
PIP	0.048	0.042	0.034	0.045	0.065	0.049	0.042	0.057
MCP	0.109	0.117	0.065	0.101	0.129	0.123	0.111	0.078

Table 4
Intra- and inter-person variability of \underline{M}^{max} ($\times 10^{-3}$ N m)

	Intra-person variability				Inter-person variability			
	Digit				Digit			
	2	3	4	5	2	3	4	5
DIP	0.015	0.029	0.023	0.008	0.033	0.052	0.039	0.014
PIP	0.096	0.122	0.063	0.052	0.152	0.247	0.154	0.113
MCP	0.385	0.291	0.322	0.211	0.662	0.876	0.734	0.435

analogous to Bernstein’s ‘leading level of control’ that achieves task-relevant goals in the sensory (i.e., joint angle) subspace (Bernstein, 1996). The ‘lower-level’ control of the

musculoskeletal system involving detailed muscle synergies, automatism, and corrections (Todorov, 2004) was compactly represented by the proposed torque-driven model. The model depicts the lumped actions of the musculotendons attached to finger joints, but with fine-tuning by the \underline{M}^{\max} parameters that simulate the complex coupling and interplay between finger joint actuation mechanisms. In the functional hierarchy, the low level of neural feedback augments the dynamics of the musculoskeletal system, while the high level controls the dynamical system ‘ensemble’ to achieve presumed optimality with objectives such as minimum energy consumption (Alexander, 1997) or torque change (Uno et al., 1989). Such a modeling approach permits a computationally efficient simulation of human movements, often difficult to achieve by the muscle-excitation-driven forward dynamic models (Pandy, 2001). A model without much neuromuscular detail can be appropriate for examining and modeling the upper-level control schemes, when the functional control at a greater scale is of investigative interest (He et al., 2001).

A parsimonious PD control without the integral component is adopted for model simplicity, but also for two additional considerations. First, it is difficult to relate the integral control to any physically meaningful aspect of human motor control process. Second, the integral control tends to add instability to the system to eliminate the steady-state error; since our model contains non-linear components such as torque limit ratios, incorporating integral component into the feedback controller would cause instability in the system or irregular behavior of the response.

The proposed model allows distinction between the variability in control strategy and that in physical factors. The K^p and K^d jointly characterize the movement control strategy, whereas \underline{M}^{\max} is embedded with individual anthropometric and physiological differences. We found that the inter-person variability in K^p or K^d was comparable to the intra-person variability, whereas the inter-person variability of \underline{M}^{\max} was on average about twice as large as the intra-person variability. This suggests that despite the anthropometric and physiological (i.e., the “plant”) differences across individuals, there is some degree of uniformity in the normative neuromotor control of multi-finger movements. Hand functional impairment of a neurological cause may be manifested as changes in associated parameters, more likely so than that of a physical or physiological cause. A more extensive application of the proposed model, accompanied by an analysis of the model parameters, featuring symptomatic and asymptomatic comparisons may lead to quantitative clinical assessment criteria and tools.

Two limitations of the current work are noted. First, the computational advantage of the torque-actuated model is enjoyed with the absence of the musculotendon components. A model with the musculotendon details to ascertain the muscle and tendon forces that produce the required torques is underway (Zhang et al., 2007). Preliminary

results indicate the estimated peak forces are within the same order of magnitude (<10 N) as previously model-predicted (Brook et al., 1995; Buchner et al., 1988; Sancho-Bru et al., 2001) or measured in vivo (Dennerlein et al., 1999; Kurasa et al., 2006), thus lending some credence to the torque profiles resulting from the current study. Second, while the modeling scheme is believed to be general, the estimated model parameters and associated interpretations are specific to the movements studied here. It is anticipated that a change in the movement (e.g., different types of grasp) or force system (e.g., when there is an external force applied at the finger-tip) would lead to a different set of model parameters and possibly new interpretations and insights.

Conflict of interest

None.

Acknowledgments

This work was supported by the National Science Foundation (DMI-0200143). The authors also wish to thank Peter Braido and Kang Li for their technical assistance.

Appendix A. Supplementary data

Supplementary data associated with this article can be found in the online version at [10.1016/j.jbiomech.2007.04.021](https://doi.org/10.1016/j.jbiomech.2007.04.021).

References

- Alexander, R.M., 1997. A minimum energy cost hypothesis for human arm trajectories. *Biological Cybernetics* 76, 97–105.
- An, K.N., Chao, E.Y., Cooney, W.P., Linscheid, R.L., 1979. Normative model of human hand for biomechanical analysis. *Journal of Biomechanics* 12, 775–788.
- Anderson, F.C., Pandy, M.G., 2001. Dynamic optimization of human walking. *Journal of Biomechanical Engineering* 123, 381–390.
- Bernstein, N.A., 1996. *On Dexterity and its Development*. Lawrence Erlbaum Associates, Mahwah, NJ.
- Braido, P.N., Zhang, X., 2004. Quantitative analysis of finger motion coordination in hand manipulative and gestic acts. *Human Movement Science* 22, 661–678.
- Brook, N., Mizrahi, J., Shoam, M., Dayan, J., 1995. A biomechanical model of index finger dynamics. *Medical Engineering and Physics* 17, 54–63.
- Buchholz, B., Armstrong, T.J., 1992. A kinematic model of the human hand to evaluate its prehensile capabilities. *Journal of Biomechanics* 25, 149–162.
- Buchner, H.J., Hines, M.J., Hemani, H., 1988. A dynamic model for finger interphalangeal coordination. *Journal of Biomechanics* 21, 459–468.
- Darling, W.G., Cole, K.J., Miller, G.F., 1994. Coordination of index finger movements. *Journal of Biomechanics* 27, 479–491.
- Delp, S.L., Loan, J.P., 2000. A computational framework for simulating and analyzing human and animal movement. *IEEE Computing in Science and Engineering* 2, 46–55.
- Dempster, W.T., 1955. Space requirements of the seated operator. WADC-TR-55-159, Aerospace Medical Research Laboratories,

- Wright-Paterson Air Force Base, OH (as cited in Chaffin, D.B., Andersson, G.B.J., Martin, B.J., 1999. *Occupational Biomechanics*. Wiley, New York).
- Dennerlein, J.T., Diao, E., Mote Jr., C.D., Rempel, D.M., 1999. In vivo finger flexor tendon force while tapping on a keyswitch. *Journal of Orthopaedic Research* 17, 178–184.
- Gottlieb, G.L., Agarwal, G.C., 1979. Response to sudden torques about the ankle in man: myotatic reflex. *Journal of Neurophysiology* 42, 91–106.
- Hatsopolous, N.G., 1994. Is a virtual trajectory necessary in reaching movements? *Biological Cybernetics* 70, 541–551.
- He, J., Maltenfort, M.G., Wang, Q., Hamm, T.M., 2001. Learning from biological systems: modeling neural control. *IEEE Control Systems Magazine* 21, 55–69.
- Holguin, P.H., Rico, A.A., Gomez, L.P., Munuera, L.M., 1999. The coordinate movement of the interphalangeal joints: a cinematic study. *Clinical Orthopaedics and Related Research* 362, 117–124.
- Kamper, D.G., Hornby, T.G., Rymer, W.Z., 2002. Extrinsic flexor muscles generate concurrent flexion of all three finger joints. *Journal of Biomechanics* 35, 1581–1589.
- Kuo, P.L., Lee, D.L., Jindrich, D.L., Dennerlein, J.T., 2006. Finger joint coordination during tapping. *Journal of Biomechanics* 39, 2934–2942.
- Kursa, K., Lattanza, L., Diao, E., Rempel, D., 2006. In vivo flexor tendon forces increase with finger and wrist flexion during active finger flexion and extension. *Journal of Orthopaedic Research* 24, 763–769.
- Lee, S.-W., Zhang, X., 2005. Development and validation of an optimization-based model for power-grip posture prediction. *Journal of Biomechanics* 38, 1591–1597.
- Li, Z.M., Zatsiorsky, V.M., Latash, M.L., 2000. Contribution of the extrinsic and intrinsic hand muscles to the moments in finger joints. *Clinical Biomechanics* 15, 203–211.
- Milner, T.E., Dhaliwal, S.S., 2002. Activation of intrinsic and extrinsic finger muscles in relation to the finger tip force vector. *Experimental Brain Research* 146, 197–204.
- Pandy, M.G., 2001. Computer modeling and simulation of human movement. *Annual Review of Biomedical Engineering* 3, 245–273.
- Pearlman, J.L., Roach, S.S., Valero-Cuevas, F.J., 2004. The fundamental thumb-tip force vectors produced by the muscles of the thumb. *Journal of Orthopaedic Research* 22, 306–312.
- Sancho-Bru, J.L., Perez-Gonzalez, A., Vergara-Monedero, M., Giurintano, D., 2001. A 3D dynamic model of human finger for studying free movements. *Journal of Biomechanics* 34, 1491–1500.
- Sancho-Bru, J.L., Perez-Gonzalez, A., Vergara-Monedero, M., Giurintano, D., 2003. A 3D biomechanical model of the hand for power grip. *Journal of Biomechanical Engineering* 125, 78–83.
- Todorov, E., 2004. Optimality principles in sensorimotor control. *Nature Neuroscience* 7, 907–915.
- Uno, Y., Kawato, M., Suzuki, R., 1989. Formation and control of optimum trajectory in human multijoint arm movement—minimum torque-change model. *Biological Cybernetics* 61, 89–101.
- Valero-Cuevas, F.J., Zajac, F.E., Burgar, C.G., 1998. Large index-fingertip forces are produced by subject-independent patterns of muscle excitation. *Journal of Biomechanics* 31, 693–703.
- Winter, D.A., 2004. *Biomechanics and Motor Control of Human Movement*, third ed. Wiley, New York.
- Zhang, X., Chaffin, D.B., 2005. Digital human modeling for computer-aided ergonomics. In: Karwowski, W., Marras, W.S. (Eds.), *Handbook of Occupational Ergonomics*. Taylor & Francis, CRC Press, London, Boca Raton.
- Zhang, X., Li, K., Vakis, A., 2007. Biological inspiration from dynamic modeling of human hand and trap-jaw ant mandible movements. In: *Proceedings of the XXI Congress of International Society of Biomechanics*, Taipei, Taiwan.